Cent. Eur. J. Geosci. • 5(4) • 2013 • 480-496
DOI: 10.2478/s13533-012-0147-2

VERSITA

Central European Journal of **Geosciences**

Eruptive history of the Barombi Mbo Maar, Cameroon Volcanic Line, Central Africa: Constraints from volcanic facies analysis

Research Article

Boris Chako Tchamabé[1,2*], Dieudonné Youmen[2], Sébastien Owona[2], Issa[1,4], Takeshi Ohba[1], Károly Németh[5], Moussa Nsangou Ngapna[2], Asobo N. E. Asaah[3], Festus T. Aka[4], Gregory Tanyileke[4], Joseph V. Hell[4]

1 *Laboratory of Volcanology and Geochemistry, Department of Chemistry, Tokai University, 4-1-1 Kitakaname, Hiratsuka, Kanagawa, 259-1292 Japan*

2 *Department of Earth Science, Faculty of Sciences, University of Douala, PO Box 24157 Douala-Cameroon*

3 *Department of Earth and Planetary Sciences, Tokyo Institute of Technology, Meguro-ku, 12-18, 2-12-1 Ookayama, Tokyo 152-8551, Japan*

4 *Institute of Mining and Geological Research (IRGM), PO Box 4110, Yaoundé, Cameroon*

5 *CS-IAE, Volcanic Risk Solutions, Massey University, Private Bag 11222, Palmerston North, New Zealand*

Received 12 June 2013; accepted 1 October 2013

Abstract: his study presents the first and detail field investigations of exposed deposits at proximal sections of the Barombi Mbo Maar (BMM), NE Mt Cameroon, with the aim of documenting its past activity, providing insight on the stratigraphic distribution, depositional process, and evolution of the eruptive sequences during its formation. Field evidence reveals that the BMM deposit is about 126m thick, of which about 20m is buried lowermost under the lake level and covered by vegetation. Based on variation in pyroclastic facies within the deposit, it can be divided into three main stratigraphic units: U_1, U_2 and U_3. Interpretation of these features indicates that U_1 consists of alternating lapilli-ash-lapilli beds series, in which fallout derived individual lapilli-rich beds are demarcated by surges deposits made up of thin, fine-grained and consolidated ash-beds that are well-defined, well-sorted and laterally continuous in outcrop scale. U_2, a pyroclastic fall-derived unit, shows crudely lenticular stratified scoriaceous layers, in which many fluidal and spindle bombs-rich lapilli-beds are separated by very thin, coarse-vesiculated-ash-beds, overlain by a mantle xenolith- and accidental lithic-rich explosive breccia, and massive lapilli tuff and lapillistone. U_3 displays a series of surges and pyroclastic fall layers. Emplacement processes were largely controlled by fallout deposition and turbulent diluted pyroclastic density currents under “dry” and “wet” conditions. The eruptive activity evolved in a series of initial phreatic eruptions, which gradually became phreatomagmatic, followed by a phreato-Strombolian and a violent phreatomagmatic fragmentation. A relatively long-time break, demonstrated by a paleosol between U_2 and U_3, would have permitted the feeding of the root zone or the prominent crater by the water that sustained the next eruptive episode, dominated by subsequent phreatomagmatic eruptions. These preliminary results require complementary studies, such as geochemistry, for a better understanding of the changes in the eruptive styles, and to develop more constraints on the maar’s polygenetic origin.

Keywords: Barombi Mbo Maar • Cameroon Volcanic Line • pyroclastic facies • phreato-Strombolian • monogenetic volcanic field.

*E-mail: boris.chako@yahoo.fr, boris.chako@gmail.com

0.1. Introduction

Maar-diatreme volcanoes, tuff rings, and tuff cones have received much attention in recent years due to their complexity and the contrasting lithofacies associated with their deposits, which offer excellent opportunities to appreciate small scale variations in magmatic processes, sustaining their formation. They are created by explosive eruptions through phreatomagmatic fragmentation of magma that occurs when rising magma interacts with groundwater, cutting the country rocks to make a deep or shallow crater, which is either dry or water-filled depending on the level of the groundwater table [1–6]. Maar-diatreme volcanoes are surrounded by a low rim of bedded pyroclastic ejecta, of several metres to over 100 m high, with a radial width of 2-5 km (when measured from the centre of the maar) [4, 6, 7]. Recent studies following a tephrostratigraphic approach have significantly enhanced our knowledge on the evolution of the tephra ring around maar craters, with an emphasis on pyroclastic facies and depositional processes [8–15] [16–22]. Research by Houghton and Hackett [23] and Martin and Németh [24] offer insights on the identification of strombolian and phreatomagmatic eruption styles, whereas [25–27] discussed the explosion mechanism, and [1], [25], [28] the quantification and control of water during fragmentation. Because they are supposed to result from single eruptive episodes and be short-lived, maar-diatreme volcanoes, tuff rings, and tuff cones had been referred to as monogenetic or "small" volcanoes ("small-volume", referring to the general small volcanic edifice volume) [1], [6]. They are, therefore, considered nowadays as one of the main volcanic landforms of monogenetic volcanic fields, especially among those areas where groundwater is abundant. However, some recent studies [19, 29, 30] demonstrated that maar deposits can perform complex, contrasting stratigraphy, and multiple eruptive styles, with evidence of short or prolonged inactivity periods between depositional units [6]. This implies that they exhibit longer eruption durations than expected [6], [31] and might be suggestive of polygenetic activity. More investigation on maars that are still poorly constrained can bring new insights on this polygenetic aspect, which also is commonly linked with polymagmatic processes.

The Cameroon Volcanic Line (CVL), a 1,600 km chain of polygenetic and monogenetic volcanoes trending N30°E from the Pagalú Island in the Gulf of Guinea to the Ngaoundéré plateau in northern Cameroon [32] (Fig. 1a), is dotted by at least 40 crater lakes [33], and some of them occupy maars. These maars are examples of poorly constrained volcanoes, due to the limited data available on them [20, 34]. Moreover, because of the 1986 catastrophic event at Nyos Maar, NW-Cameroon, a better understanding of their past volcanic history is essential for volcanic risk assessment along the CVL. This could also contribute to developing the full volcanic history of the CVL.

We carried out a careful examination of pyroclastic deposits of the Barombi Mbo Maar (BMM), Kumba plain, Cameroon (Fig. 1b). These deposits were initially presented in Cornen et al. [35] as a 100 m of volcanic materials, showing two similar series of basaltic tuff lapilli separated by a paleosol. It has been inferred that this is a tuff-ring, based on low-angle sub-horizontal stratification of the lower deposit unit that dips 10 – 15°towards the lake [35]. Indeed, this stratigraphic feature characterises a tuff ring, but a better understanding of its past activity, the main aim of this study, requires more information on the deposit characteristics. This includes the stratigraphic features and illustrations of some key pyroclastic facies, representation of the stratigraphy distribution and main depositional processes presented in this paper. On the basis of deposit characteristics, we draw preliminary hypotheses on the main eruptive styles and an overview of the general eruptive history during the BMM formation.

1. Geological background

The BMM is located 3 km NW of Kumba Town, between 4°N38'55"-4°N40'15" and 9°E23'30"-9°E24'46" in the Kumba plain (Fig. 1b). It is filled by the largest crater lake of the CVL. The lake, of the same name, is 306 m a.s.l., with a mean diameter of about 2.5 km and a depth of 111 m [35]. According to Dumort [36], the BMM is the youngest of a series of three W–E nested coalescing maars, cutting through the Pan-african Granito-gneissic substrate and overlain by Cretaceous to Cenozoic sandstones [34, 37]. However, a DEM of the BMM area (Fig. 1c), realized by digitalizing a cartographic map of the area with MapInfo software and further constructing the 3D surface model in Surfer8, was produced to depict this coalescing aspect. The BMM and three others maars: the Barombi Koto, Mbwadong and Dissoni in the Kumba Plain[1], were formed during the period of activity represented by the second of the three main volcanic features identified therein: (1) old basaltic lavas covering the entire plain; (2) cinder cones and phreatomagmatic units; and (3) short vesicular basaltic lava flow, well rep-

[1] *linkt to Google map:* https://maps.google.com/maps/ms?msid=200066345236377165163.0004e482e80a4eee4afd8&msa=0&ll=4.82826,9.31778&spn=0.942828,0.484772&iwloc=0004e482f6612964b4017

resented in the north of the BMM [34, 35]. These activities probably began in the Eocene [36] and completed 1Ma ago [35]. Excluding investigations of some pioneers involved in palynology and limnology [33, 35], a detailed geological study of the Kumba Plain is lacking. Fig. 1b presents an updated version of the geological map of the BMM vicinity, modified after [35–37].

2. Methods

2.1. Fieldwork

The BMM deposit was examined at many sites in the vicinity of Lake Barombi Mbo (Fig. 1b) for characterization and identification of its different pyroclastic facies. The deposit rises 100m above the lake level and has steep walls mostly covered by moss. It was, therefore, not able to be accessed in its entirely, reducing the main descriptions to proximal sections, where some deposits features are displayed. Beds and layers were described, and lithofacies recorded, using a combination of grain size, bed thickness, fabric, structures, relative sorting, grading pattern, lithification, unconformities, and sedimentary features and the relative juvenile to lithic pyroclasts ratio according to [8–19], [29, 38]. Determination of clasts sizes, shapes, types, and abundances were limited to qualitative appreciations. Layers were differentiated from one another by their contrasting internal characteristics. Correlation of closer beds or layers allowed the construction of a stratigraphy log (Fig. 2) from the bottom to the top of the deposit.

2.2. Terminology

In this study, individual beds are referred to as very thin to thick beds, according to Sohn and Chough [10] (i.e., thickness of 1 cm to 1 m), whereas layers with thickness >1 m, consist of many thin and medium beds. A unit is a sum of two or more layers. Thicknesses are referred herein as a measurement in centimetres or metres in the brackets in front of beds, layers or unit codes. For example, L_{1a} (2.5 m) means layer L_{1a} is 2.5 m thick. Eruptive unit and eruptive episode are used here to define pyroclastic deposits bounded by a paleosol, considered as representing a prolonged time of inactivity [29, 30]. Eruptive sequence corresponds to a single eruption, within which many eruptive phases or eruptive styles can occur, each one emplacing a single depositional layer/bed [30]. Descriptive terms of tephra and pyroclastic rocks are those commonly used and proposed in [17, 39], and [40].

3. Results and interpretations

3.1. Field aspect

The BMM tuff ring forms around Lake Barombi Mbo a horseshoe-shaped rim with a circumference of about 14 km. The DEM of the BMM area (Fig. 1c) shows a scar of a probable old maar, west of the BMM. Therefore, instead of three coalescing craters, as suggested by [36], only two are observed. This scar defines an approximate area closer to that of the actual Lake Barombi Mbo. According to Fig. 2 in [35], and considering the Lake Barombi Mbo as a truncated cone, the lake will have a surface of about 4.9 km^2 and a base surface of 0.78 km^2, with a volume of about 1.13 km^3. Assuming that the old maar had a similar or even a smaller depth than that of the actual Lake Barombi Mbo, it would have hosted such an important volume of water.

GPS measurements (handheld GARMIN GPSMAP62s) from the lowest point where the deposit appears to the summit suggest that the tuff ring is about 126 m thick. The deposit wall is exceptionally steep. It does not show any obvious zonation, either in colour or structure, when observed from a certain distance, as do some maar tuff rings (e.g., the Narbona Pass Maar, Mexico in USA [19]. This absence of zonation might be due to the impact of excessive moisture on the deposits generated by the evergreen forest. Upon close inspection, a noticeable difference in clast size, type and shape, bed thickness, unconformities, relative sorting, grading pattern, lithification and other sedimentary structures within the deposits could be distinguished, allowing it to be sub-divided into three main stratigraphic units (U_1, U_2, and U_3) (Fig. 2). The lower part of the stratigraphic succession displays parallel and sub-planar-beds 5 to 25 cm thick (Fig. 3), similar to that of the upper part. Many disorganised and structureless lithic-rich layers are also found in the second and upper units, and their thicknesses vary from 1 to 3 m. Clast size increases from U_1 to U_2, and tends to diminish at the summit of the deposit. Clast types in beds or layers also vary from lithic-rich to lithic and juvenile mixed, and juvenile-rich. The juvenile clasts are usually dense and less vesicular, mainly presenting cauliflower to oval bomb shapes in U_2 and U_3.

3.2. Stratigraphic units and associated pyroclastic facies

The three main stratigraphic units distinguished initially on the basis of their general stratifications each contain one or many of the volcanism related facies [15, 16] described in this section and interpreted in terms of depo-

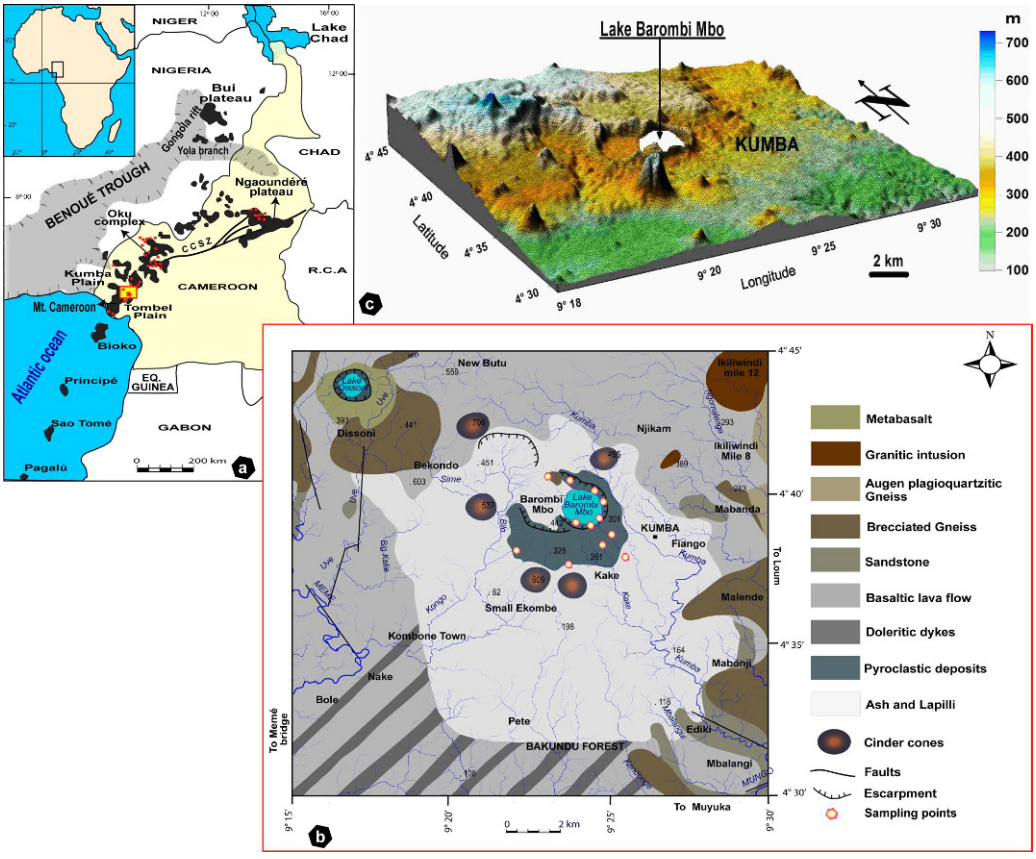

Figure 1. Map of the Study area. a) Location of the BMM along the Cameroon Volcanic Line (see the yellow rectangle). The red points are crater lakes. b) Geological map of the Kumba Plain, modified after [35, 36], and [37]. c) 3D view of the BMM vicinity showing the scar of an ancient maar at its west side.

sitional processes. The pyroclastic lithofacies identified, and the stratigraphic logs of the BMM deposit, are summarized in Fig. 2.

Unit 1 (U_1)

Because ca. 21 m of U_1 (26 m) is buried below the lake level and colonized by vegetation, its description is restricted to its upper part L_1 (5 m). L_1 was sub-divided into two sub-layers: L_{1a} and L_{1b} (Fig. 2). Deposits locally outcropping at the lower part presented similar stratification and inclination as observed in layer L_{1a}.

L_{1a} (2.5 m) displays a series of parallel bedded, thinly stratified and alternating coarse- and- fine clast-supported beds, dipping sub-horizontally, with a bedding inclination range of 13-15°(Fig. 3a, e). All single beds are well-defined, laterally continuous and do not present any basal scour features. Coarse-grained beds are lapilli-rich (5 – 25 cm) and are unconsolidated, loosely packed, well sorted and essentially composed of lithic fragments. Juvenile clasts are apparently absent from these beds except for one 20 cm thick bed, consisting exclusively of highly vesiculated scoria, which appears almost at the top of the bed series forming L_{1a}, i.e., at about 21.5 m from the "basal" part of the deposit (Fig. 3a, b). The lapilli-rich beds are bounded by matrix-supported tuff beds (5–10 cm) that are also dominated by fine lithic clasts (Fig. 3c, d). All these tuff beds are consolidated and well sorted.

L_{1b} (2.5 m) displays at its lower part thinly to very thinly bedded tuff, relatively planar, slightly undulated and almost coherent (Fig. 3e). This lamination continues up to the top of the layer, but becomes disturbed and wavier, showing low-undulatory stratified beds (Fig. 3f). This part is poorly sorted, and from a visual estimation of the bulk mass of clast contents, is composed of 60% lapilli and 40% ash. The transition to layer L_2 (U_2) is marked by a simple variation in particle sizes (Fig. 3g), with the clast size increasing gradually from lapilli up to blocks and bombs, forming a reverse grading. Some tree moulds are visible therein, however, because they are totally decayed, no charcoal was found in the mould.

***Interpretation*:** Alternating bedding, in which single lapilli-rich beds are demarcated by thin fine ash-fall layers, with all beds mantle-bedded, well-defined and well-

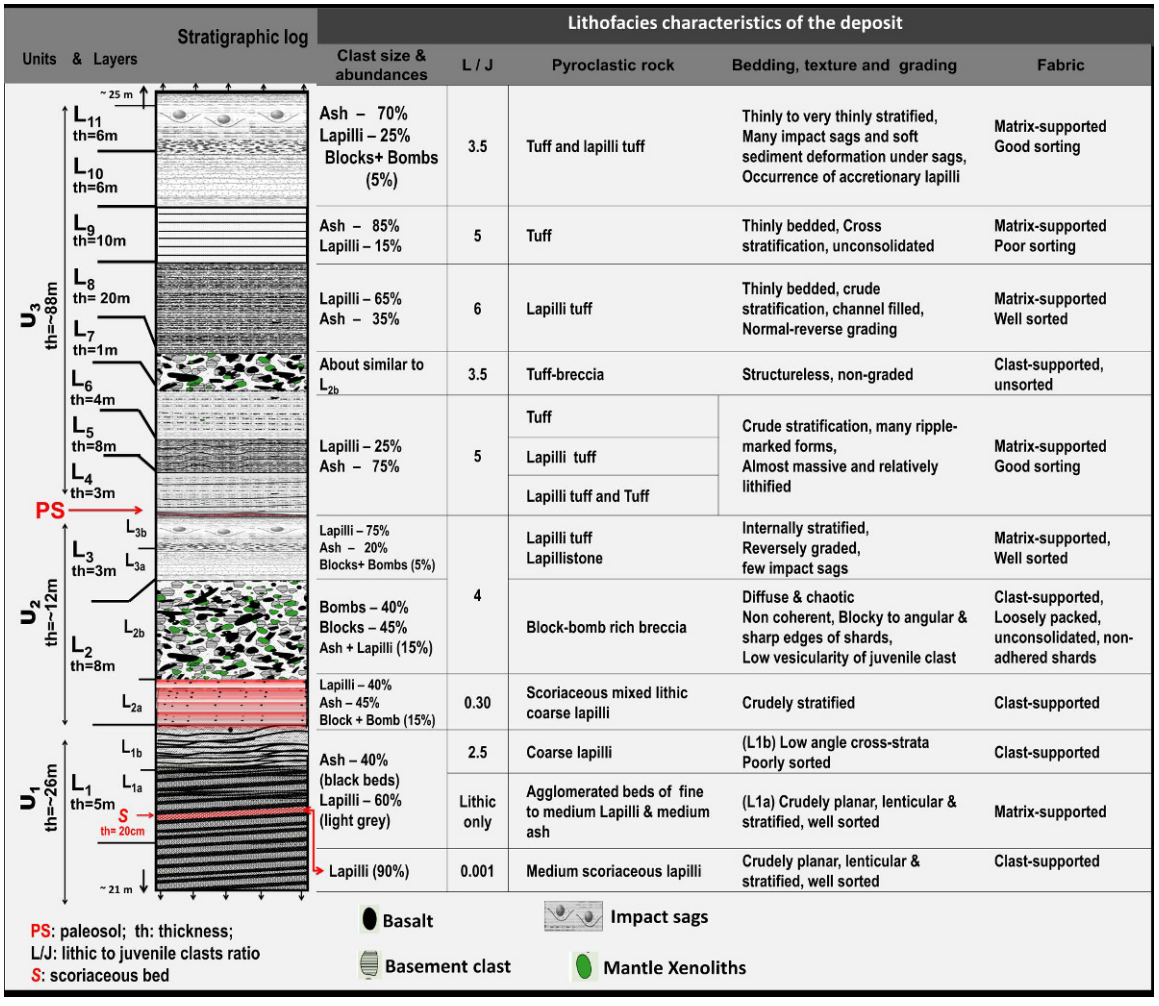

Figure 2. Summary of the general features and stratigraphy of the phreatomagmatic deposits of the BMM. The stratigraphic scale is not respected. The lithic to juvenile ratio (L/J) is calculated as a simple ratio of approximate percentage of lithic and juvenile clasts in layers or beds.

sorted, as presented by L_{1a}, reflects a typical deposition from pyroclastic fall. Moreover, due to the lateral continuity of the bed series, their good sorting and the low bedding inclination, L_{1a} may correspond to deposition from a surge that was probably segregated into different eddies or organised into a turbulent and high-concentration head followed by a lower concentrated tail [10]. Similar stratification was identified in the basaltic phreatomagmatic deposit of the Peña Mountain (West Texas) and also ascribed to deposition from high-concentration deflating base surges, in which rapid suspension sedimentation prevented tractional reworking of particles [42]. However, the presence of unconsolidated and consolidated beds indicates that L_{1a} is a succession of dry fall deposits (Fig. 3a, b) and wet fall deposits (Fig. 3d) intercalated with wet surge deposition as shown by the fine-matrix supported tuff (Fig. 3c).

The slight undulation and important cohesive appearance of particles to beds at the lower part of L_{1b} suggest that the deposition was under "wet" conditions [9, 15], whereas its upper part - with low-angle stratification and slightly wavy bedding and unconsolidated - reflects deposition of turbulent dilute pyroclastic density current from a "dry" surge.

Unit 2 (U_2)

U_2 (~12 m) displays two successive layers, L_2 and L_3 that are recognizable by their changes in particle sizes and clast- and matrix-supported aspect respectively. L_2 (8 m) is diffusively stratified and chaotic. Its bottom, L_{2a} (3 m), is scoriaceous, well to moderately sorted, clast-supported and weakly bedded. It presents crude and lenticular stratification, with normally to inversely graded lapilli-beds separated by very thin coarse-ash-beds (Fig. 4a). The lapilli lenses consist mainly of poorly vesiculated scoria,

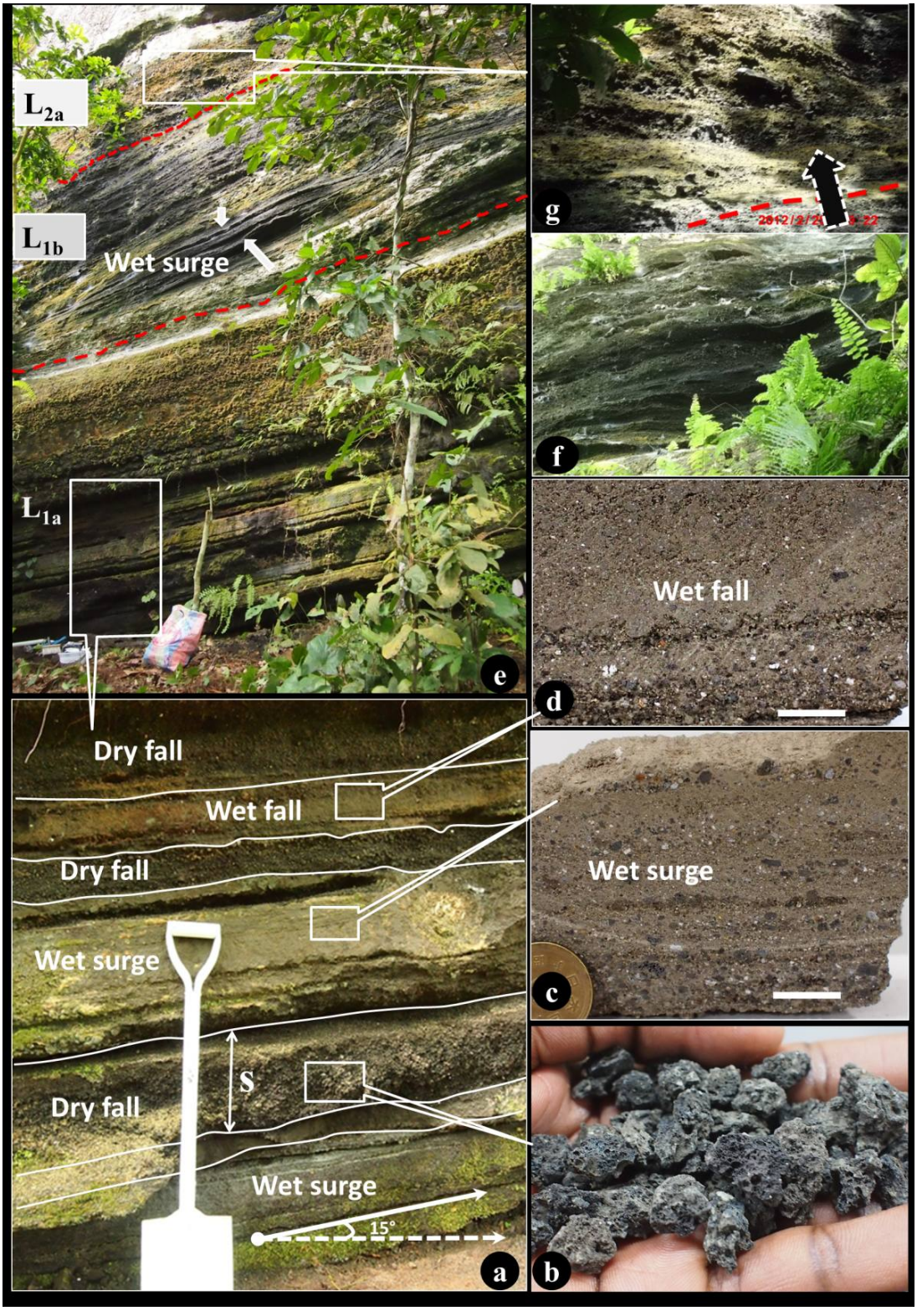

Figure 3. Some key pyroclastic features of Unit U_1. a) Series of parallel and thinly stratified and alternating coarse and fine grain-supported beds. The thin scoria-rich bed of Fig. 2 is represented here by (S). b) Vesicular scoria in a coarse lapilli bed in layer L_{1a}. c) and (d) are polished blocky samples from ash-rich beds of the first layer. Note the enrichment in lithic (white particles) and cognate angular black particles. The scale bar is 2 cm. e) Thinly and stratified alternating beds are displayed at the lower part, while the middle part shows thinly bedded lapilli tuff. Bed surfaces are slightly undulatory (arrows). f) Disturbed and slightly wavy stratification showing low-undulation. g) Transition between L_{1b} and L_{2a} marked by simple variation in particles sizes and types, increasing gradually from poorly vesicular lapilli up to blocks and bombs.

dense juvenile clasts and angular lithic-rich cauliflower bombs. Many spindle and fluidal bombs (Fig. 4b, c) are also found in this layer, and accidental lithic fragments are present but in very low proportions.

L_{2b} (5 m) is lithic-rich, massive and clast supported. It is structureless, disorganized, unsorted to poorly sorted, containing abundant angular to sub-rounded blocks and lapilli that are heterogeneous in composition (Fig. 4d). The juvenile clasts here are dense with very low vesicularity. They are mainly cauliflower and breadcrust bombs. Clast proportion consists of about 15% of coarse ash and lapilli, and 85% for blocks and bombs. 80% of clasts are angular with sharp edges. L_3 (3 m) is compact, matrix-supported and fully consolidated, with beds strongly adhered together (Fig. 4e). It mantles the upper surface of L_{2b} and is characterized by an inverse grading, with a high percentage of lapilli at the top and ash at the bottom. Its lower part, L_{3a} (1.5 m), consists of about 75% of ash and 25% of lapilli in a stratified-bedded lapilli tuff, presenting some "empty" scours. Particles at the top part (L_{3b}) are more lithified, forming a lapillistone bed in which rare impact sags represent shallow penetration on the substrate, and no sedimentary related deformation (Fig. 4f).

Interpretation: L_{2a} characteristics might be indicative of particle accretion from different pulses developed within a pyroclastic density current (PDC), in which lapilli lenses recorded the coarse grained part of the PDC, whereas the stratified coarse ash recorded the more dilute part accompanying each pulse [18]. Also, rapid deposition from dense suspension in the granular-fluid-based PDC with subsequent tractional transport would have been possible [10, 11, 41]. Such stratification was found in scoria cones in Western Mexico and Central Libya [24], and was interpreted as resulting from repeated explosions driven by magmatic degassing in an open conduit, because of the scoriaceous nature of the beds. Hence, we suggest that L_{2a} might have resulted from this style of activity.

L_{2b} characteristics suggest deposition by rapid sedimentation of clasts from a high concentration suspension of ash and lapilli, in which the rate of supply was higher than the rate of deposition, and also that there was no or little tractional processes [10, 15, 16, 18, 19, 29]. Its structureless, poorly sorted and mantle bedding aspect confirms a pyroclastic fall origin [12], whereas its position near the base unit of the tuff ring, the abundance of heterogeneous angular to sub-round blocks and lapilli, the low vesicularity of juvenile clasts and abundance of cauliflower bombs are indicative of an explosion breccia-derived phreatomagmatic fall out [1].

L_3, which appears to be more compact, matrix supported and well consolidated to highly lithified, and has occasional impact sags, reflects a depositional process by particle sedimentation with ballistic projectiles during settling [20, 29]. However, concentration of fine lapilli tuff at the bottom (L_{3a}) and lapillistone (L_{3b}) at the top indicate that there would have been elutriation of fine particles during transportation [10].

Unit 3 (U_3)

U_3 (topmost unit) constitutes the greatest part of the deposits and consists of many disorganised and well-stratified layers piled up repetitively to about 90 m in thickness. U_3 is separated from U_2 by a thin layer (10 cm) of exposed paleosol. Immediately on-top of the paleosol, at about 346 m in elevation, the bottom of U_3 (L_4) presents roughly the same characteristics as L_3. L_4 (3 m) is massive, well sorted, crudely stratified and consists of successive matrix-supported and well-graded lapilli tuff (15–25 cm), separated by very thin (2–4 cm) and lithified tuff, presenting symmetric to asymmetric climbing ripples forms (Fig. 5a, b). L_4 is overlain by a more lithified layer, L_5 (8 m) that presents almost similar facies as L_4. However, it is more deformed, and the ripples structures are coarser and show soft-loading deformation (Fig. 5c). On-top of this, L_6 (4 m) shows a stratified to crudely stratified massive matrix supported tuff. Rare blocks are observed, and no juvenile clasts were found therein. It is followed (going upwards) by L_7, a disorganized clast-supported massive lapilli layer, containing abundant blocks of lithic (Fig. 5d, e), similar to L_{2b}.

Further upwards, at about 378 m height, L_8 (20 m) shows a monotonous succession of stratified lapilli tuff (Fig. 6a). It is globally clast-supported, moderately sorted, and characterised by thin beds of few millimetres to up to 25 cm in thickness. It displays planar stratified beds, laterally continuous with distinct trains of lapilli. Many channels filled by lapilli-rich lithic clasts are available through the layer (Fig. 6b). Lapilli-rich beds are clast-supported, massive, and occasionally reversely graded.

At 400 m height, L_9 (10 m) consists of very thinly to lenticular crudely stratified tuff, overlain by a reworked deposit, which shows planar and low-angle cross-stratification. The lower part of L_9 has beds with cross-laminated tuff, characterized by thin, discontinuous and lenticular sets of lens (Fig. 6c, d). The layer is entirely matrix-supported, and clasts of lapilli size are scarcer here.

L_{10} consists of a sequentially alternating, highly lithified tuff and poorly sorted and unconsolidated lapilli-rich beds. The lithified tuff beds are extremely thinly to crudely stratified and locally undulating or displaying cross-stratification. They are matrix supported and sprinkled with many impact sags and some infilling sedimentary feature patterns, such as mantle-bedding. Their thickness varies between 10 and 40 cm. Lapilli beds are internally stratified and almost inversely or normally

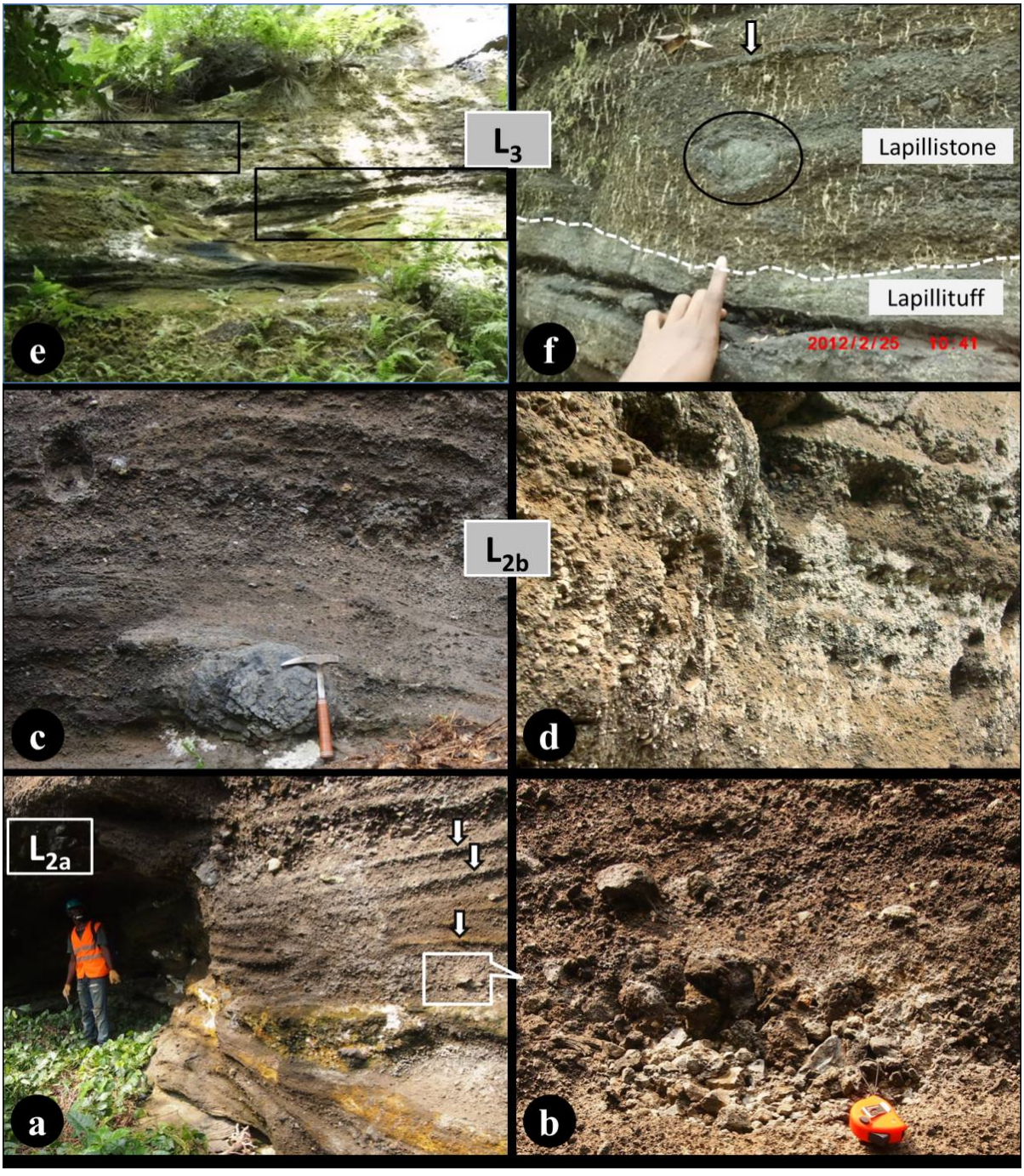

Figure 4. Unit U_2 and its facies. a) Crudely stratified, and normal to inversely graded lapilli-beds separated by very thin lens of coarse ash-beds (arrows). b) Close view of the lapilli beds showing angular clasts and sub-rounded scoria almost oxidized. c) Fluidal basaltic bomb at the bottom of layer L_{2b}. (d) a disorganized, unconsolidated and unsorted clast supported tuff-breccia. Clast size is dominantly lapilli, and crevices are where mantle xenoliths or juvenile fragments have often been removed by students or researchers. e) Low-angle wavy and very thinly stratified bedded lapillituff covered by moss. The stratification can be observed in the rectangular boxes. f) Close view of the upper part of layer L_3, showing a compact, and matrix supported and highly lithified lapillituff and lapillistone. Note the presence of very thin beds of fine ash (see arrows) strongly adhered to the lapillistone bed and the open cracks or scours (see the hand) in the lapillituff. Note also a low penetration impact sag in the lapillistone circle).

graded. They are accidental lithic-rich, containing centimetre to decimetre size blocks of basement rock, and also many peridotites and pyroxenites xenoliths (Fig. 7a, b).

L_{11} at the top almost presents the same stratification pattern as L_{1a} (unit U_1). It is made of a series of paralleled thinly stratified and alternating medium and fine grain-supported beds (Fig. 7c). All the single beds are well-defined, laterally continuous and do not present any traction at their contact surface. They are internally laminated, lithified, containing many accretionary lapilli, impact sags and mud-cracks structures (Fig. 7d, e, f). About 25 m of the upper part of deposit is not described here.

Interpretation: Layers L_4 and L_5 and L_6 of Unit 3 present similar stratification patterns, but differ only by their consolidation level. As they present massive, well-sorted, crudely stratified beds and consist of successive matrix-supported and well graded lapilli tuff separated by very thin and lithified tuff, they can be interpreted as originating from a "wet" pyroclastic surge or a low particle concentration PDC [10].

The monotonous succession of alternating stratified lapilli tuff and tuff with indistinct and continuous lapilli trains observed in L_8 can be interpreted as being emplaced by suspension and traction sedimentation from a turbulent base surge, which fluctuates in velocity and particle concentration following the observations of [11] within the base surges of the Sohgaksan tuff ring. This might also be indicative of emplacement by a combination of PDC and surge fallout-derived pulsating phreatomagmatic explosions, as documented elsewhere [19]. The thick and crude stratification, the poor sorting and the presence of occasional inverse grading with lapilli tuff beds suggest deposition of rapid suspension sedimentation from an unsteady, high-concentration PDC with little traction, whereas the presence of several discontinuous lithic clast-trains, and occurrence of lapilli lithic-rich filling channels/pockets, is indicative of a relatively slow sedimentation rate and even with the little traction during transport [11, 15].

Based on the thinly bedded aspect of L_9, showing planar stratification and low-angle cross-stratification (Fig. 6), it can be interpreted as being generated by a "wet" pyroclastic surge [9], containing a relatively low particle concentration, turbulent current, which had lost some of its particle load by sedimentation and tractional transport [11]. The alternating lithified massive tuff and unconsolidated poorly sorted lapilli-rich beds in L_{10} suggest subsequent deposition of a different mechanism. Unconsolidated and disorganized lapilli tuff beds that are internally slightly stratified and almost inversely or normally graded demonstrate either rapid deposition, or hindered settling with buoyancy and dispersive pressure provided by shearing mass suspension with little traction [11]. The lithified tuff beds, thinly and crudely stratified, locally undulated or displaying cross-stratification and sprinkled with many impact sags and some infilling sedimentary features such as mantle-bedding, typically represent deposition from a PDC in "wet" conditions accompanied by ballistic projection [15].

Layer L_{11} has, as L_{1a}, a series of paralleled thinly stratified and alternating medium and fine grain-supported beds, with single beds being well-defined, laterally continuous and presenting no traction at their surface, also suggesting deposition from a surge. However, in contrast to L_{1a} in which the deposition was under dry conditions, the presence of accretionary lapilli, mud-cracks and impact sags in L_{11} typically suggest that it was deposited under wet conditions [19, 43], probably by gentle settlement of particles from steam-rich phreatomagmatic eruption columns [15, 18], or from convecting pyroclastic surge clouds in which there was abundant moisture and/or continuous vapour condensation [11].

4. Discussion

4.1. Eruptive history of the BMM

The various facies described above and interpreted as representing different depositional mechanisms indicate that the BMM is the record of a complex, multiphase eruptive styles (Fig. 8) during which the supply of water had a significant influence during fragmentation and deposition. Characteristics of L_{1a} were interpreted as a succession of dry and wet fall deposits, intercalated with wet surges. In its alternating succession of lapilli-ash-lapilli bed series, almost all beds were fine and accidental grained lithic-rich, apart from the 20cm thick scoriaceous beds. This indicates that eruptive activities at the BMM would have started with phreatic eruptions. Based on Fig. 1c, and assuming that the old maar west of the BMM was water-filled, rising magma would have vaporized this water-saturated zone beneath the water-filled old maar, favouring a phreatic eruption. The explosion itself would have likely had the force to displace and partially vaporize the old lake.

The presence of the thin lapilli-rich scoria bed between L_{1a} beds and the high vesicularity of its juvenile clasts (Fig. 3a, b), suggest that the water-supply stopped after a short time and/or the magma-supply rate may have been increased, leading to an intermittent magmatic fragmentation of successful magma batches that were able to penetrate through the water-saturated zones. Therefore, fragmentation would have been sustained by magmatic volatile pressure [8], vesiculation and partial fragmentation

Figure 5. Unit U_3 and its facies. a) b) and c) show a monotonous succession of thin trains of ash and lapilli tuff. The ash trains display climbing current-ripple forms similar to that shown on Fig. 5b in [41]. (d) Massive matrix supported and structureless layer, overlain by e) a disorganized, unsorted clast-supported layer.

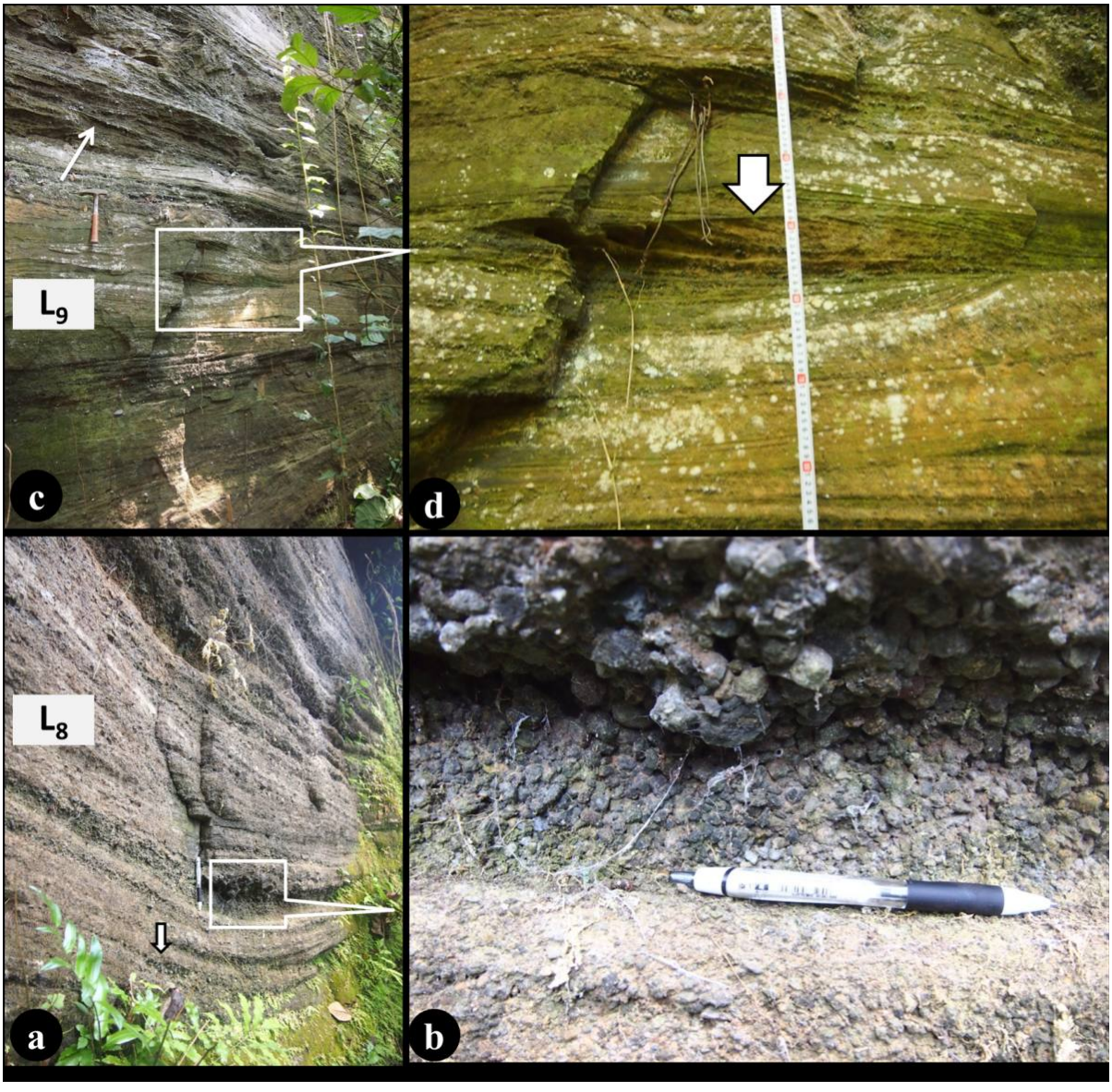

Figure 6. Unit U_3 and its facies (continued). a) Monotonous succession of crudely stratified lapilli tuff layer showing the occurrence of channels filled by lithic clasts (b). c) Very thinly stratified surge layer. (d) shows cross stratification in the surge layer. Stoss-side (feature arrow) can be observed.

of magma, as compared to the formation of a similar scoria bed in the Keanakakoi Ash deposit Member (Kilauea volcano) [29]. L_{1b} was deposited subsequently by "wet" and "dry" surges conditions. A mixture of accidental lithic and juvenile clasts therein indicates that the phreatic activities (L_{1a}) were followed by a phreatomagmatic explosion.

After U_1, the stratigraphy consisted of the juvenile bomb-, block- and accidental lithic-rich L_2, laying directly on L_{1b} with no evidence of an erosional limit. Such mixing of juveniles and lithic clasts in a pyroclastic deposit are known to represent a phreatomagmatic eruption. However, the higher concentration of scoriaceous and dense (spindle and fluidal bomb) juvenile clasts, and few lithic clasts at its lower part (L_{2b}), is indicative of a more complex fragmentation regime [13]. Therefore, we suggest that water probably became intermittently exhausted, giving rise to repeated explosions, driven by magmatic degassing and phreatomagmatic explosions which we qualify as phreato-Strombolian activity. This qualification might match up with Stárková et al. [44] who suggested the same conclusion for such a mixture, characterized by the presence of scoria fragments and accretionary lapilli in an armoured

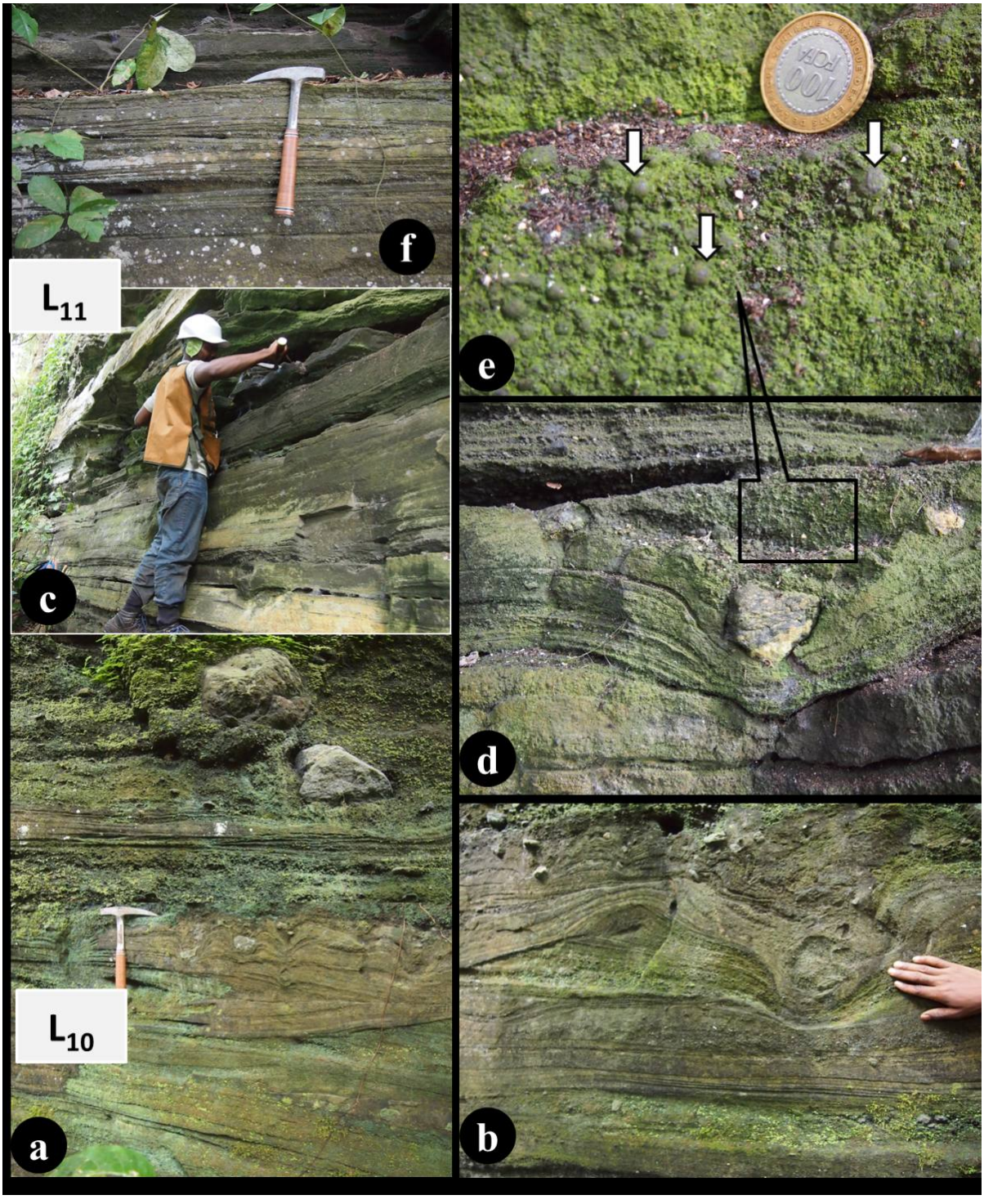

Figure 7. Unit U_3 and its facies (continued). a) Successions of lithified and unconsolidated beds. Note the occurrence of many impact sags and soft sedimentary deformation under impact sags (a) and (b). c) Series of parallel beds relatively consolidated and containing accretionary lapilli (e). The coin is 2.3 cm width. f) shows thinly stratified surge deposit with mud crack structures at the top.

lapilli bed found in the Levín Volcanic Field (Czech Republic). The abundance of lithic fragments, their angular morphology and the relatively low degree of vesicularity of the juvenile clasts in the upper part (L_{2b}) suggest that the fragmentation process was dominated by phreatomagmatic activity. Moreover, the importance of lithic clasts indicates significant quarrying of the vent zone [43, 45, 46] due to an energetic phreatomagmatic explosion. The style of phreatomagmatic fragmentation and the resulting eruption can be highly influenced by the host rock environment (e.g., hard or soft rock) through which the magma must penetrate [5, 47, 48]. Occurrences of accidental lithic granite, diorite, gneiss and cognate basaltic fragments in L_{2b} also reveal that the shock wave released by the magma-water interaction would have been significantly enough to fragmenting the granite-gneissic basement in the Kumba plain during this eruptive phase. This stage could be related to the opening of the BMM prominent crater, after which explosions continuously produced ash and lapilli fall to form layer L_3. However, for such a phreatomagmatic fragmentation to occur after a dry phreato-Strombolian explosion, another supply of water was necessary. We suggest that a short repose period allowed the re-establishment of the conditions necessary to produce phreatomagmatic activity.

On cessation of phreatomagmatic explosions, the first of the two main volcanic episodes was completed. The presence of paleosol (~10 cm) at the end of this series is proof of a relatively long period of inactivity before the second eruptive episode that sustained the deposition of U_3 [30]. This is because the formation of soils, even if it depends on the type of soil or on the area they are found, requires at least 1Ma [49].

Regarding descriptions provided for layers in U_3, it is likely that eruptive activities were governed by subsequent phreatomagmatic fragmentations in dry and mostly wet conditions. This observation corroborates perfectly with the occurrence of many sedimentary structures, such as current-ripple forms in L_4 and L_5, and soft deformations of beds under impact sags, mud cracks and abundant accretionary lapilli observed in L_{10} and L_{11}. Therefore, we assume that during the period of inactivity meteoric water filled the prominent crater, and concomitantly, cracks developed in the basement rock during the first explosions would have progressively favoured the feeding of the root zone by groundwater [5, 15], permitting the development of the second volcanic episode. This second eruptive sequence subsequently involved many phreatomagmatic explosions. Regarding the various unconsolidated and lithified layers, it is clear that water-supply was also intermittent, but permanent, to avoid formation of pure magmatic explosions.

4.2. First evidences of polygenetic activity

Monogenetic volcanoes are typically considered as erupting only once due to their limited magma supply [50]. On the other hand, polygenetic volcanoes possessing a large magma storage chamber erupt repeatedly [51] and consequently deposit materials that can display distinct eruptive units. Volcanoes located in plains along the CVL have been considered as monogenetic [32], but field evidence suggests that the BMM cannot perfectly fit the monogenetic definition. This is because: (1) the thickness (126 m) of the deposit and the several distinct layers that are indicative of repeated eruptions; (2) as repetition is one of the main characteristics of monogenetic hydromagmatic eruptions with the continuous entry/depletion of water in the conduit, some short repose period for water recharge may be required between explosions to change from a magmatic-dominated style (Phreato-Strombolian) to a phreatomagmatic one (Fig. 8); and (3) the presence of the paleosol (~10 cm) provides evidence of long repose periods and ultimately suggests that the BMM had a long eruptive duration with at least two main eruptive episodes (Fig. 8) [6, 31]. In addition, the repeated explosions with different eruptive styles indicates that there would have been a relatively large store of magma beneath the BMM.

5. Conclusions

Preliminary investigations of pyroclastic deposits around the BMM, Kumba Plain, Cameroon Volcanic Line, were performed with the purposes of providing information on its stratigraphy, the main depositional process and eruptive sequences during its formation. Field evidence shows that the BMM pyroclastic ejecta is about 126 m thick. Based on the variations in bed thickness, fabric, structures, relative sorting, grading pattern, lithification, clasts sizes and the juvenile to lithic pyroclasts ratio in individual beds, unconformities and other sedimentary features, deposits were subdivided into three deposit units, U_1, U_2, and U_3, piled up successively with respective thicknesses of about 26 m, 13 m and 87 m. U_1, at the bottom of the outcrops, was incompletely described due to weathering and vegetation.

The thickness (126 m) of the deposit, and the evidence of short and long repose periods (paleosol) between the stratigraphic units, strongly suggest that the BMM is a polygenetic volcano. There were two major volcanic episodes with a complex eruptive evolution, involving variable eruptive styles and fall out deposition and turbulent diluted pyroclastic density currents. In view of the various deposits features and pyroclastic facies observed, water would have significantly influenced the fragmentation and

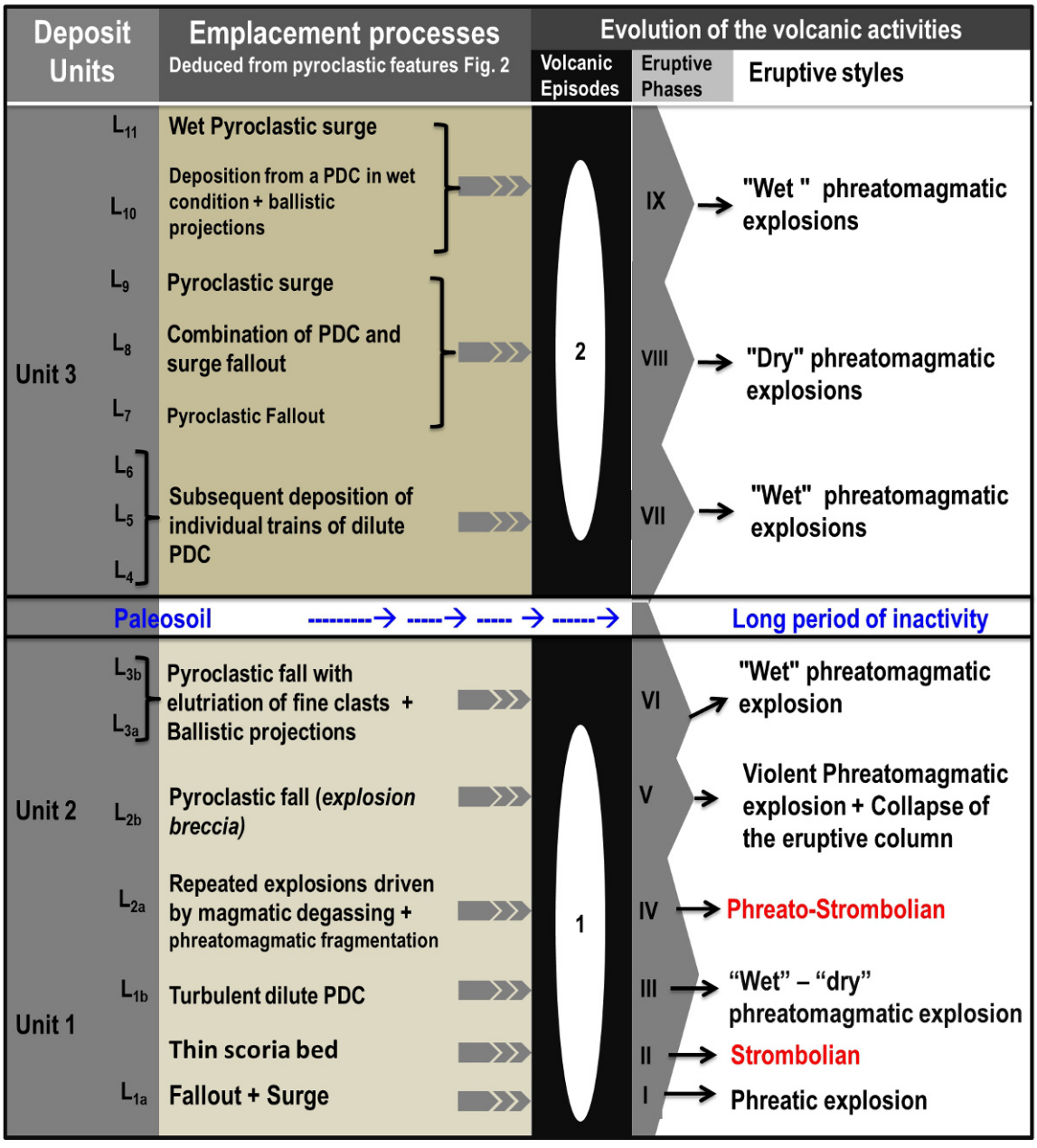

Figure 8. Summary of the depositional mechanism and the main volcanic activities. The Emplacement processes are deduced from the interpretation of pyroclastic facies (see text) and the main structures displayed by the deposits.

depositional processes during the volcanic activities. The sequence of eruptive activities was phreatic – Strombolian – phreatomagmatic – phreato-Strombolian – phreatomagmatic explosions. However, geochemical data and morphoscopic analyses of juvenile clasts from the subsequent layers of the three units are required for further explanation and constraint on the polygenetic aspect as suggested by [2].

Acknowledgements

This research was funded by the SATREPS-IRGM Project titled "Magmatic Fluid Supply into Lakes Nyos and Monoun, and Mitigation of Natural Disasters through capacity building in Cameroon". The Leader of this project, namely Prof. Takeshi OHBA and his team, are greatly thanked for initiating this prestigious and qualitative

project, useful to forecast volcanic events from crater lakes in Cameroon. The authors would like to address many thanks to all the anonymous reviewers for their constructive comments, and especially to Dr. Dmitri Rouwet. Careful reading and comments on the manuscript by Dr Kate Arentsen made the text more focused and clear.

References

[1] Wohletz K.H., Shéridan M. F., Hydrovolcanic explosion II: Evolution of tuffs rings and tuff cones. *Am. J. Sci.*, 1983, 283, 385-413

[2] Lorenz V., On the formation of Maars. *Bull. Volcanol.*, 1973, 37, 183-204

[3] Lorenz V., Formation of phreatomagmatic maar-diatreme volcanoes and its relevance to kimberlite diatremes. *Phys. Chem. Earth.*, 1975, 9, 17-27

[4] Lorenz V., Maars and Diatremes of phreatomagmatic origin: A Review. *Trans. Geol. Soc. S.Afr.*, 1985, 88, 459-470

[5] Lorenz V., Maar-Diatreme Volcanoes, their Formation, and their Setting in Hard-rock or Soft-rock Environments. *GeoLines*, 2003, 15, 72-83

[6] White J.D.L., Ross P.-S., Maar-diatreme volcanoes: A review. *J. Volcanol. Geotherm. Res.*, 2011, 201, 1-29

[7] Lorenz V., Syn- and post-eruptive hazards of maar-diatreme volcanoes. *J. Volcanol. Geotherm. Res.*, 2007, 159, 285-312

[8] Cas R.A.F., Wright J. V., Volcanic successions: modern and ancient. Allen & Unwin, London, 1987.

[9] Valentine G.A., Stratified flow in pyroclastic surges. *Bull. Volcanol.*, 1987, 49, 616-630

[10] Sohn Y.K., Chough S.K., Depositional processes of the Suwolbong tuff ring, Cheju Island (Korea). *Sedimentol.*, 1989, 36, 837-855

[11] Chough S.K., Sohn Y.K., Depositional mechanics and sequences of base surges, Songaksan tuff ring, Cheju Island, Korea. *Sedimentol.*, 1990, 37, 1115-1135

[12] Valentine G.A., Giannetti B., Single pyroclastic beds deposited by simultaneous fallout and surge processes: Roccamonfina volcano, Italy. *J. Volcanol. Geotherm. Res.*, 1995, 64, 129-137

[13] White J.D.L., Schmincke H.-U., Phreatomagmatic eruptive and depositional processes during the 1949 eruption on La Palma canary Islands. *J. Volcanol. Geotherm. Res.*, 1999, 94, 283-304

[14] Dellino P., La Volpe L., Structures and grain size distribution in surge deposits as a tool for modelling the dynamics of dilute pyroclastic density currents at La Fossa di Vulcano aeolian Islands, Italy). *J. Volcanol. Geotherm. Res.*, 2000, 96, 57-78

[15] Németh K., Martin U., Harangi Sz., Miocene phreatomagmatic volcanism at Tihany (Pannonian Basin, Hungary). *J. Volcanol. Geotherm. Res.*, 2001, 111, 111-135

[16] Németh K., White J.D.L., Reconstructing eruption processes of a Miocene monogenetic volcanic field from vent remnants: Waipiata Volcanic Field, South Island, New Zealand. *J. Volcanol. Geotherm. Res.*, 2003, 124, 1-24

[17] Németh K., Martin U., Practical volcanology-lectures notes for understanding volcanic rocks from field based studies. László Kordos, Budapest, 2007

[18] Sulpizio R., Mele D., Dellino P., La Volpe L., Deposits and physical properties of pyroclastic density currents during complex Subplinian eruptions: the AD 472 (Pollena) eruption of Somma-Vesuvius, Italy. *Sedimentol.*, 2007, 54, 607-635

[19] Brand B.D., Clarke A.B., Semken S., Eruptive conditions and depositional processes of Narbona Pass Maar volcano, Navajo volcanic field, Navajo Nation, New Mexico (USA). *Bull. Volcanol.*, 2009, 71, 49-77

[20] Ngwa C.N., Suh C.E., Devey C.W., Phreatomagmatic deposits and stratigraphic reconstruction at Debunscha Maar (Mt Cameroon volcano). *J. Volcanol. Geotherm. Res.*, 2010, 192, 201-211

[21] Murtagh R.M., White J.D.L., Sohn Y.K., Pyroclast textures of the Ilchulbong'wet' tuff cone, Jeju Island, South Korea. *J. Volcanol. Geotherm. Res.*, 2011, 201, 385-396

[22] Gernon T.M., Upton B.G.J., Hincks T.K., Eruptive history of an alkali basaltic diatreme from Elie Ness, Fife, Scotland. *Bull. Volcanol.*, 2013, 75, 1-20

[23] Houghton B.F., Hackett W.R., Strombolian and phreatomagmatic deposits of Ohakune craters, Ruapehu, New Zealand: a complex interaction between external water and rising basaltic magma. *J. Volcanol. Geotherm. Res.*, 1984, 21, 207-231

[24] Martin U., Németh K., How Strombolian is a "Strombolian" scoria cone? Some irregularities in scoria cone architecture from the Transmexican Volcanic Belt, near Volcán Ceboruco, (Mexico) and Al Haruj (Libya)., *J. Volcanol. Geotherm. Res.*, 155, 2006, 104-118

[25] Kokelaar P., Magma-water interaction in sub aqueous and emergent basaltic volcanism. *Bull. Volcanol.*, 1986, 48, 275-289

[26] Wohletz K.H., Explosive magma-water interactions: Thermodynamics, explosion mechanisms, and field studies. *Bull. Volcanol.*, 1986, 48, 245-264

[27] Wohletz K.H., Zimanowski B., Physics of phreatomagmatism. *Terra Nostra*, 2000, 6, 515-523

[28] Sheridan M.F., Wohletz K.H., Hydrovolcanic explo-

sions: the systematics of water-pyroclast equilibration, *Sciences.*, 1981, 212, 1387-1389

[29] McPhie J., Walker G.P.L., Christiansen R.L., Phreatomagmatic and phreatic fall and surge deposits from explosions at Kilauea volcano, Hawaii, 1790 A.D.: Keanakakoi Ash Member. *Bull. Volcanol.*, 1990, 52, 334-354

[30] Giordano G., Facies characteristics and magma–water interaction of the White Trachytic Tuffs (Roccamonfina Volcano, southern Italy). *Bull. Volcanol.*, 1998, 60, 10-26

[31] Németh K., Monogenetic volcanic fields: Origin, sedimentary record, and relationship with polygenetic volcanism. *Geol. Soc. Am.*, 2010, 470, 43-66

[32] Sato H., Aramaki S., Kusakabe M., Hirabayashi J.-I., Sano Y., Nojiri Y., Tchoua F., Geochemical difference of basalts between polygenetic and monogenetic volcanoes in the central part of the Cameroon volcanic line. *Geochem. J.*, 1990, 24, 357-370

[33] Kling G.W., Comparative limnology of lakes in Cameroon, West Africa. PhD thesis, Duke University, 1987

[34] Tamen J., Nkoumbou C., Mouafo L., Reusser E., Tchoua F.M., Petrology and geochemistry of monogenetic volcanoes of the Barombi Koto volcanic ?eld (Kumba Graben, Cameroon volcanic line): Implications for mantle source characteristics. *C. R. Géosci.*, 2007, 339, 799-809

[35] Cornen G., Bandet Y., Giresse P., Maley J., The nature and chronostratigraphy of Quaternary pyroclastic accumulations from Lake Barombi-Mbo (West Cameroon). *J. Volcanol. Geotherm. Res.*, 1992, 51, 357-374

[36] Dumort J.-C., Geologic map and explicative note on the Douala-west and 1/500000 map of geologic recognisance. *Dir. Min. Géol. Cam. BRGM Paris*, 1968. (In French)

[37] Teitchou M.I., Grégroire M., Dantas C., Tchoua F.M., High mantle beneath the Kumba plain Cameroon line), after spinel peridotite xenolith in basaltic lava. *C. R. Géosci.*, 2007, 33, 101-109. (In French)

[38] Valentine G.A., Perry F.V., WoldeGabriel G., Field characteristics of deposits from spatter-rich pyroclastic density currents at Summer Coon volcano, Colorado. *J. Volcanol. Geotherm. Res.*, 2000, 104, 187-199

[39] Gillespie M.R., Styles M.T., Classification of igneous rocks: BGS Rock Classification Scheme, Vol. 1. *B.G.S. R.R*, 1999, 2.

[40] White J.D.L., Houghton B.F., Primary volcaniclastic rocks. *Geol.*, 2006, 34, 677-680

[41] Kokelaar P., Raine P., Branney M.J., Incursion of a large-volume, spatter-bearing pyroclastic density current into a caldera lake: Pavey Ark ignimbrite, Scafell caldera, England. *Bull. Volcanol.*, 2007, 70, 23-54

[42] Befus K.S., Hanson R.E., Lehman T.M., Griffin W.R., Cretaceous basaltic phreatomagmatic volcanism in west Texas: Maar complex at Peña Mountain, Big Bend National park. *J. Volcanol. Geotherm. Res.*, 2008, 173, 245-264

[43] Gençalioğlu-Kuşcu G., Atilla C., Cas R.A.F., Kuşcu I., Base surge deposits, eruption history, and depositional processes of a wet phreatomagmatic volcano in Central Anatolia (Cora Maar). *J. Volcanol. Geotherm. Res.*, 2007, 159, 198-209

[44] Stárková M., Rapprich V., Breitkreuz C., Variable eruptive styles in an ancient monogenetic volcanic field: examples from the Permian Levín Volcanic Field (Krkonoše Piedmont Basin, Bohemian Massif). *J. Geosci.*, 2011, 56, 163-180

[45] Martin U., Németh K., Auer A., Breitkreuz C., Mio-Pliocene Phreatomagmatic Volcanism in a Fluvio-Lacustrine Basin in Western Hungary, *GeoLines*, 2003, 15, 84-90

[46] Németh K., Calculation of long-term erosion in Central Otago, New Zealand, based on erosional remnants of maar/tuff rings. *Z. Geomorph. N. F.*, 2003, 47, 29-49

[47] Auer A., Martin U., Németh K., The Fekete-Hegy Balaton Highland Hungary) "soft-Substrate" and "hard-substrate" maar volcanoes in an aligned volcanic complex – Implications for vent geometry, subsurface stratigraphy and the palaeoenvironmental setting. *J. Volcanol. Geotherm. Res.*, 2007, 159, 225-245

[48] Ross P.-S., Delpit S., Haller M.J., Németh K., Corbella H., Influence of the substrate on maar–diatreme volcanoes-An example of a mixed setting from the Pali Aike volcanic field, Argentina. *J. Volcanol. Geotherm. Res.*, 2011, 201, 253-271

[49] Lucas Y., Chawel A., Soil formation in tropically weathered terrains. In: Butt C.R.M. and Zeegers H., (Ed.), Regolith Exploration Geochemistry in Tropical and Subtropical Terrains, Handbook of exploration Geochemistry vol.4, *Elsevier*, 1992.

[50] Connor C.B., Conway F.M., Basaltic volcanic fields. In: Sigurdsson H., (Ed.), Encyclopedia of Volcanoes, *Academic Press*, 2000

[51] Walker G.P.L., Basaltic volcanoes and volcanic systems. In: Sigurdsson H., (Ed.), Encyclopedia of Volcanoes, *Academic Press*, 2000

[52] Németh K., An Overview of the Monogenetic Volcanic Fields of the Western Pannonian Basin: Their Field Characteristics and Outlook for Future Research from

a Global Perspective, Updates in Volcanology – A comprehensive Approach to Volcanological Problem, Prof. Francesco Stoppa, ed.), *InTech*, 2012. http://www.intechopen.com/books/updates-in-volcanology-a-comprehensive-approach-to-volcanological-problems/an-overview-of-the-monogenetic-volcanic-fields-of-the-western-pannonian-basin-their-fields-characteristics.